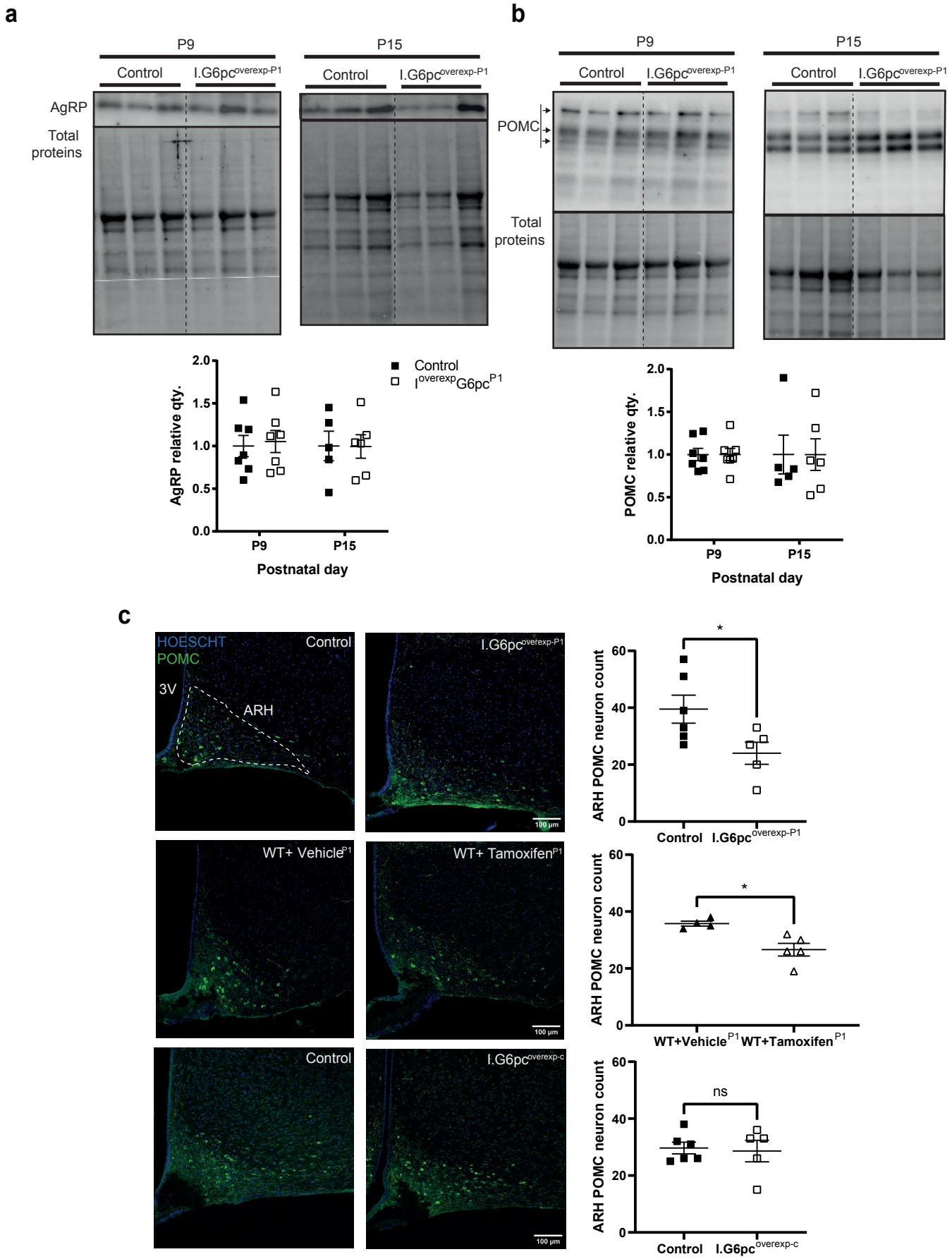


**Supplemental Fig.1 : Impact of the neonatal induction of G6pc1 on AgRP and POMC protein amount and on the number of ARH POMC neurons.**

(a-b) Representative western blot images and relative AgRP and POMC levels in the hypothalamus of I.G6pc$^{overexp\text{-}P1}$ and control pups aged of 9 and 15 days, respectively (mean ± SEM; n=5-7). (c) Representative confocal ARH images and quantification of POMC-immunoreactive cells of P20 I.G6pc$^{overexp\text{-}P1}$ and control littermates (mean ± SEM; n=5-6), P20 WT mice injected with tamoxifen or vehicle at P1 (mean ± SEM; n=4-5), and P20 I.G6pc$^{overexp\text{-}c}$ and control littermates (mean ± SEM; n=5-6). Scale bar = 100µm. P: postnatal day; 3V: 3rd ventricle; ARH: arcuate nucleus of the hypothalamus. Panels a-b: 2-way ANOVA, followed by multiple comparisons and Sidak's post hoc test; Panel c: T-tests. *p<0.05.

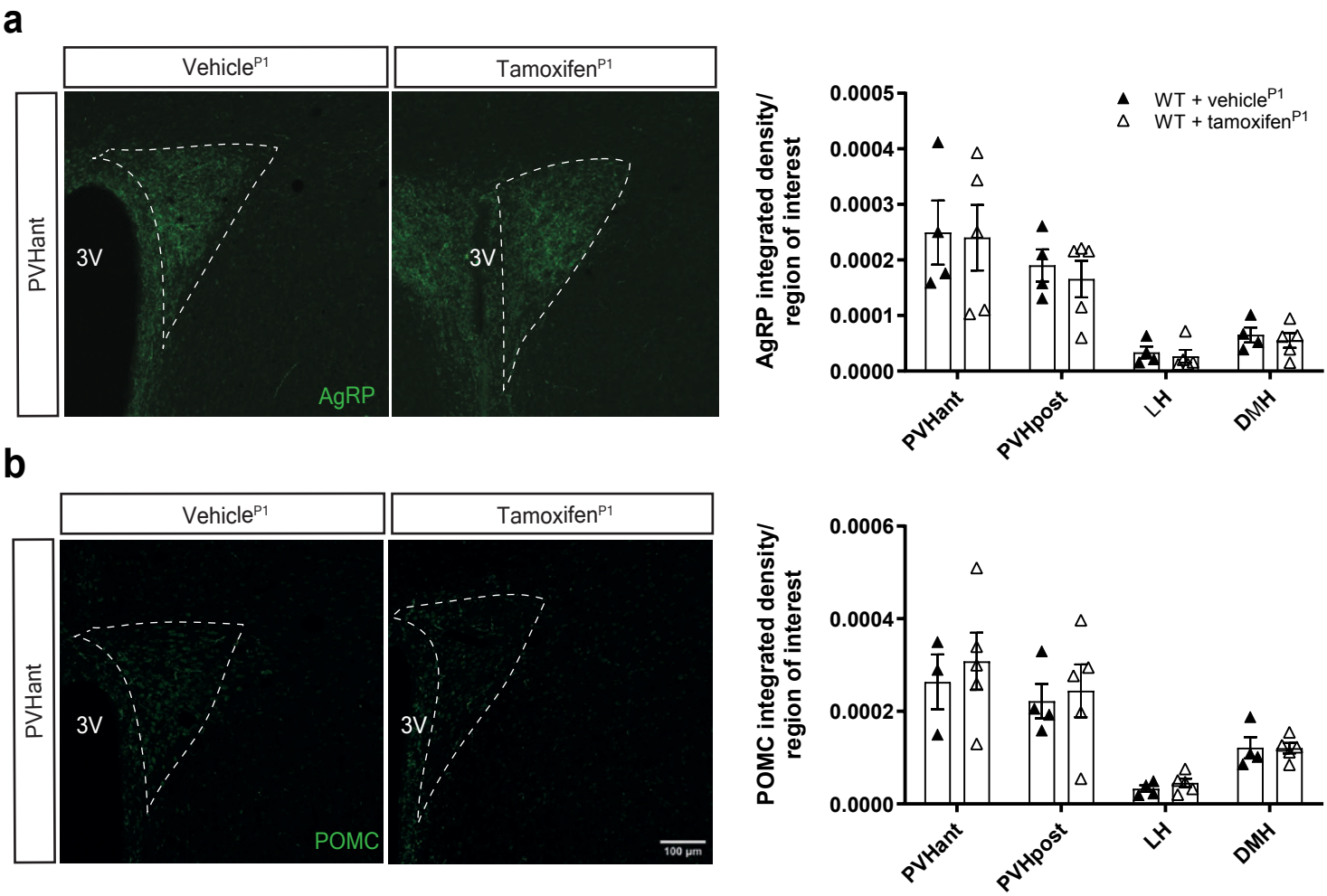


**Supplemental Fig. 2: Tamoxifen treatment of P1 pups has no effect on the development of AgRP and POMC neural projections.** (a) Representative confocal PVNant images and quantification of AgRP-immunoreactive fibers of P20 wild type pups treated with tamoxifen (white triangles) or vehicle (black triangles) at P1 (mean ± SEM; n= 4-5). (b) Representative confocal PVNant images and quantification of POMC-immunoreactive fibers of P20 wild type pups treated tamoxifen (white triangles) or vehicle (black triangles) at P1 (mean ± SEM; n= 3-5). Scale bar = 100µm P: postnatal day; 3V: 3rd ventricle; PVHant: anterior part of the paraventricular nucleus; PVHpost: posterior part of the paraventricular nucleus; LH: lateral hypothalamic area; DMH: dorsomedial nucleus. Two-way ANOVA, followed by multiple comparisons and Sidak's post hoc test were performed as statistical analyses.

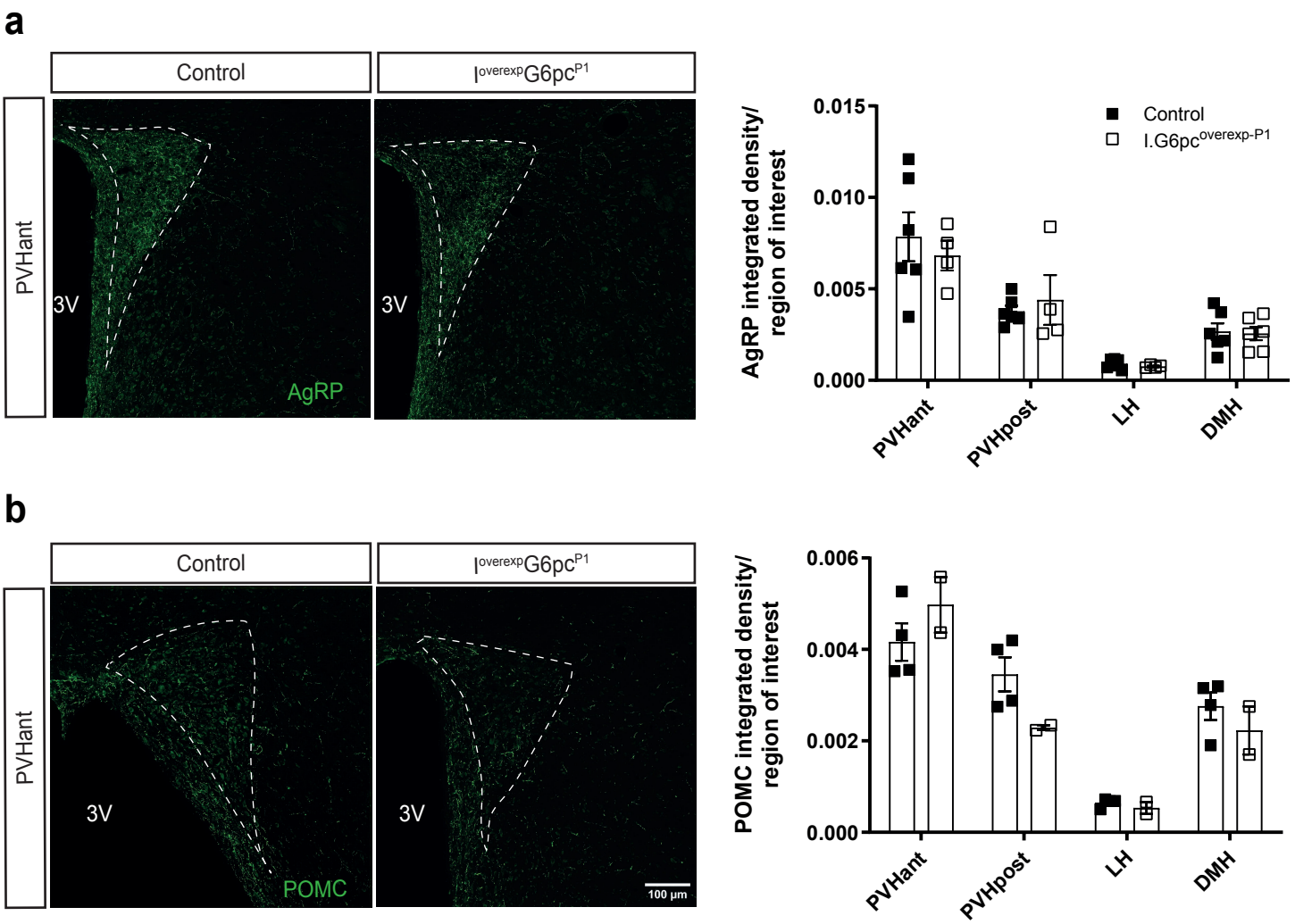


**Supplemental Fig. 3: AgRP and POMC neural projections normalized in adult I.G6pc$^{overexp-P1}$ mice.** (a) Representative confocal PVNant images and quantification of AgRP-immunoreactive fibers of P80 I.G6pc$^{overexp-P1}$ (white squares) and control littermates (black squares) (mean ± SEM; n= 5-6). (b) Representative confocal PVNant images and quantification of POMC-immunoreactive fibers of P80 I.G6pc$^{overexp-P1}$ (white squares) and control littermates (black squares) (mean ± SEM; n= 2-4). Scale bar = 100µm . P: postnatal day; 3V: 3rd ventricle; PVHant: anterior part of the paraventricular nucleus; PVHpost: posterior part of the paraventricular nucleus; LH: lateral hypothalamic area; DMH: dorsomedial nucleus. Two-way ANOVA, followed by multiple comparisons and Sidak's post hoc test were performed as statistical analyses.

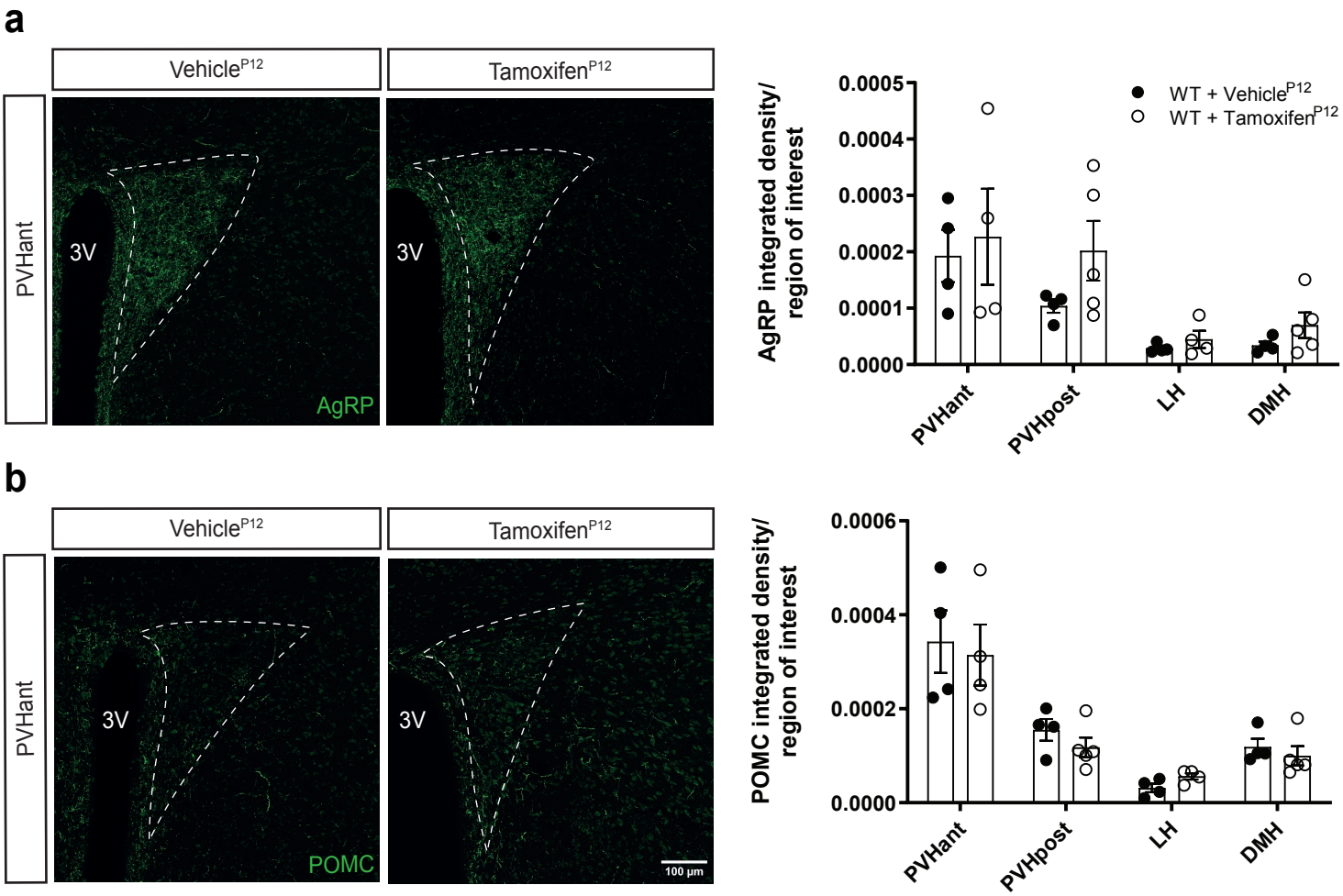


**Supplemental Fig. 4: Tamoxifen treatment at P12 has no effect on the development of AgRP and POMC neural projections.** (a) Representative confocal PVNant images and quantification of AgRP-immunoreactive fibers of P20 wild type pups treated with tamoxifen (white circles) or vehicle (black circles) at P12 (mean ± SEM; n= 4-5). (b) Representative confocal PVNant images and quantification of POMC-immunoreactive fibers of P20 wild type pups treated with tamoxifen (white circles) or vehicle (black circles) at P12 (mean ± SEM; n= 4). Scale bar = 100µm P: postnatal day; 3V: 3rd ventricle; PVHant: anterior part of the paraventricular nucleus; PVHpost: posterior part of the paraventricular nucleus; LH: lateral hypothalamic area; DMH: dorsomedial nucleus. Two-way ANOVA, followed by multiple comparisons and Sidak's post hoc test were performed as statistical analyses.

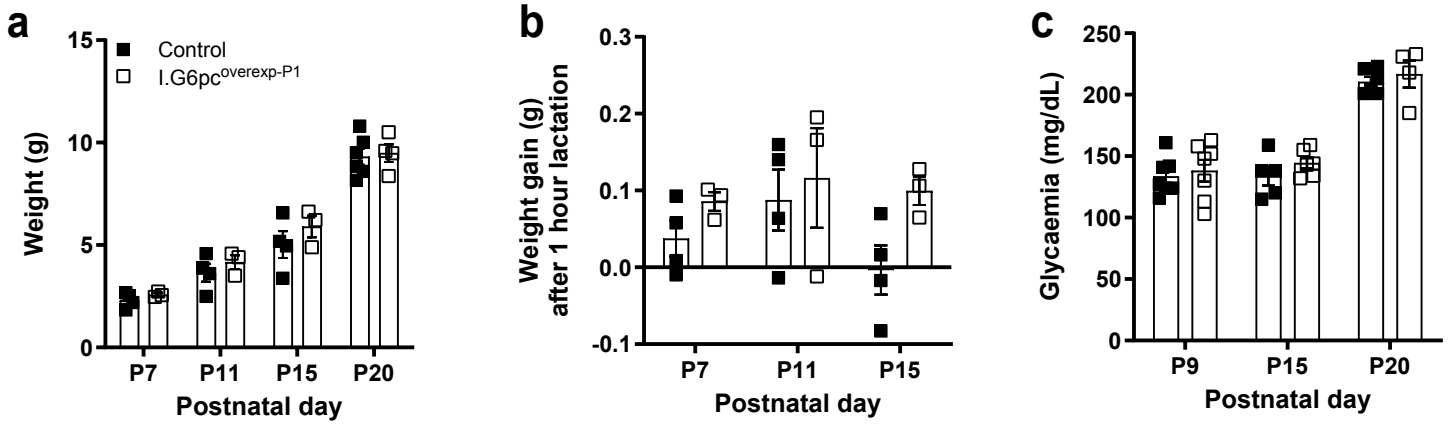


**Supplemental Fig. 5: Normal weight and glycaemia in pups with a neonatal induction of intestinal gluconeogenesis.** (a) Neonatal weight (mean ± SEM; n= 3-6). (b) Weight gain after pups were reunited with dams for 1 hour (mean ± SEM; n= 3-4). (c) Neonatal glycaemia (mean ± SEM; n= 4-7). P: postnatal day. Two-way ANOVA, followed by multiple comparisons and Sidak's post hoc test were performed as statistical analyses.

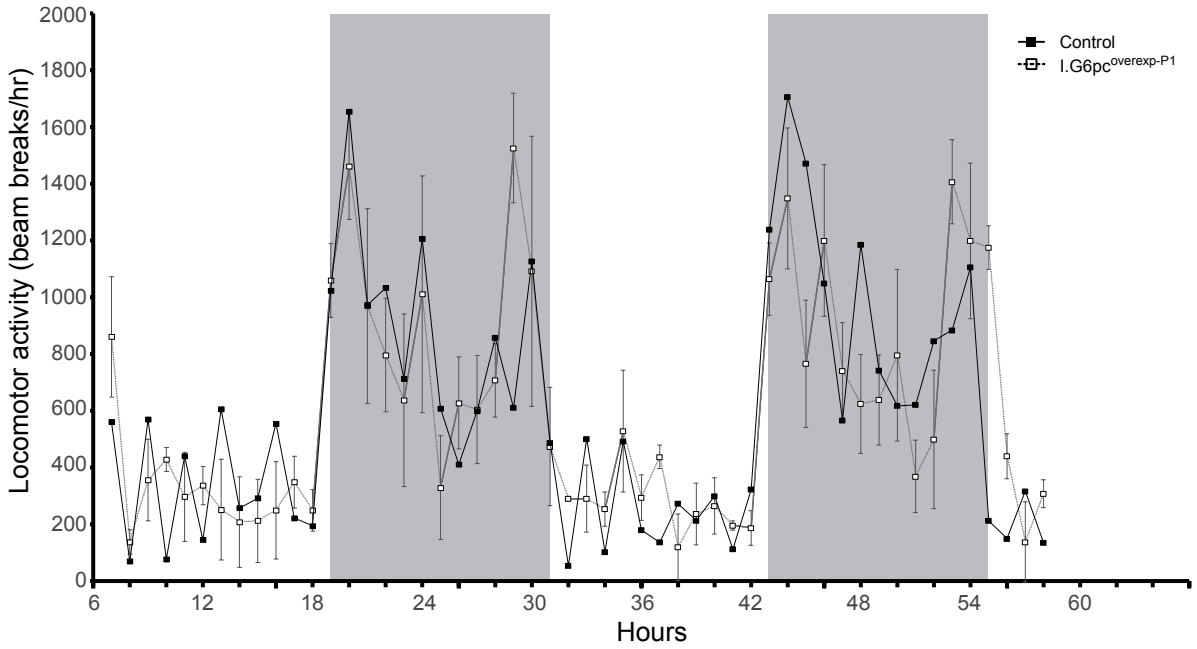


**Supplemental Fig. 6:** Hourly locomotor activity values of I.G6pc$^{overexp-P1}$ (white squares) and their control littermates (black squares) measured during the second (from 7 AM) and third day of housing in indirect calorimetric cages (mean ± SEM; n= 5-6).

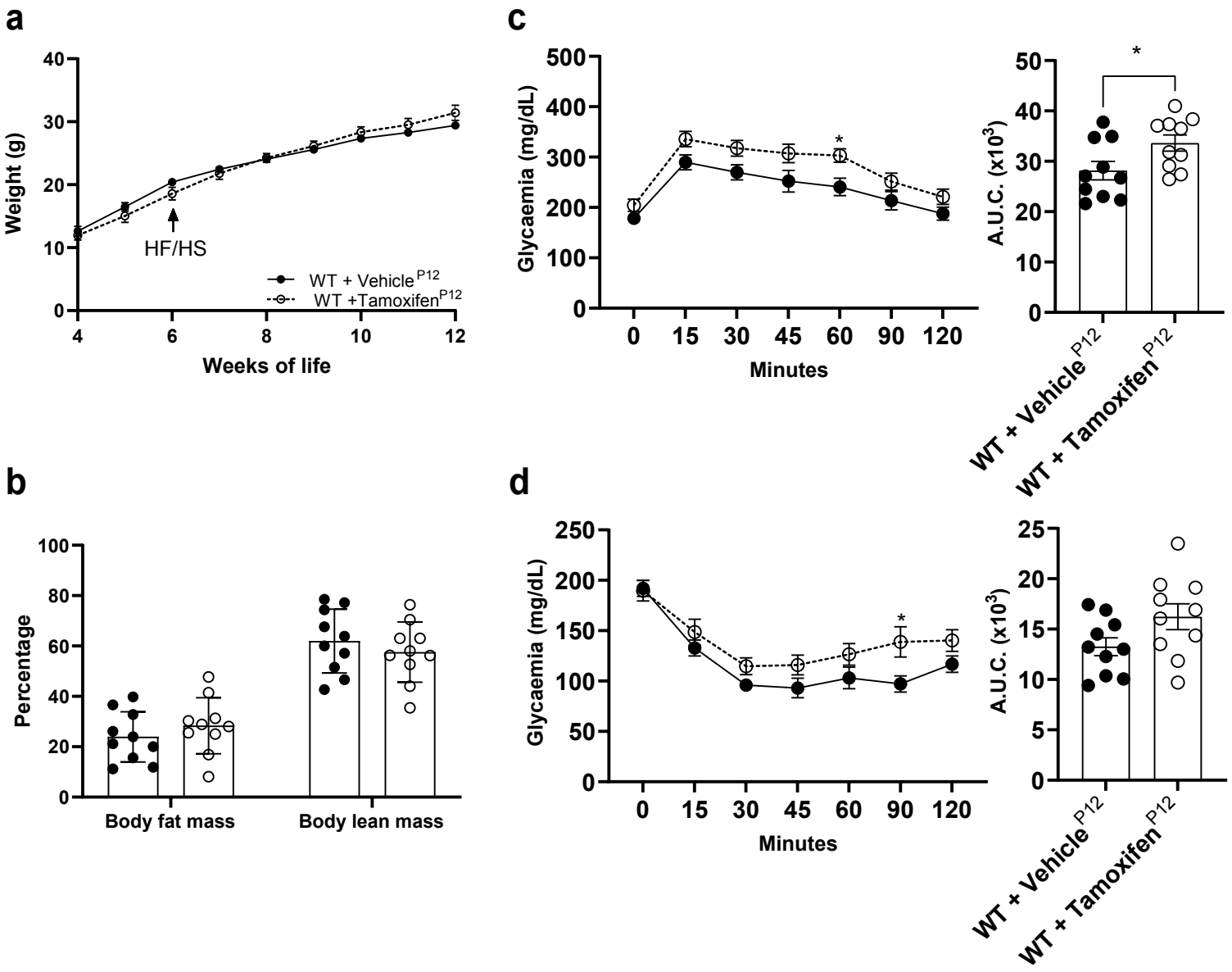


**Supplemental Fig. 7. Tamoxifen treatment at P12 has no effect on the metabolism of adult mice fed a hypercaloric diet.** Analyses were performed in adult wild-type treated with Tamoxifen (white circles) or with Vehicle (black circles) at P12 and fed a HFHS diet since the 6th week of life (mean ± SEM, n= 9-10). (a) Weight gain. (b) Body fat mass and body lean mass (% of total body weight). (c) Glucose tolerance test with corresponding AUC. (d) Insulin tolerance test with corresponding AUC. Two-way ANOVA, followed by multiple comparisons and Sidak's post hoc test were performed as statistical analyses for weight gain, glucose and insulin tolerance tests. T-tests were performed for body composition. *p<0.05.

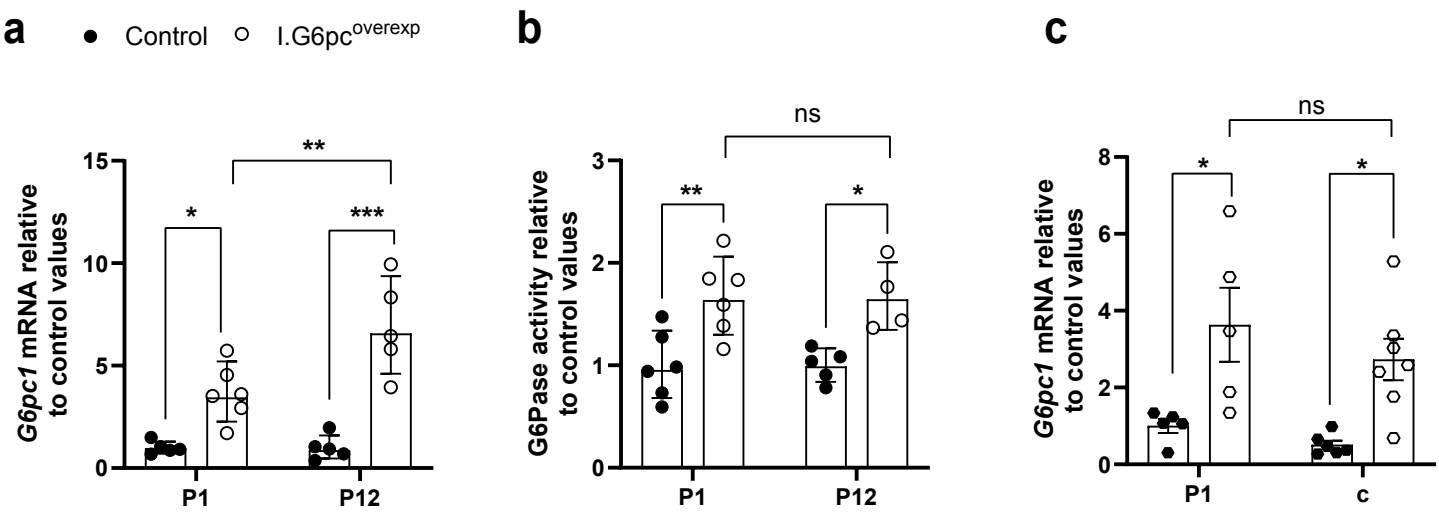


**Supplementary Fig. 8: The expression of *G6pc1* is similarly induced in the different mouse models used.** (a) Expression of *G6pc1* relative to the respective littermate values (black circles) of I.G6pc$^{overexp\text{-}P1}$ and I.G6pc$^{overexp\text{-}P12}$ mice (white circles) (mean ± SEM; n= 4-6). (b) G6Pase activity (µmol/min/g of protein) relative to the respective littermate values (black circles) of I.G6pc$^{overexp\text{-}P1}$ and I.G6pc$^{overexp\text{-}P12}$ mice (white circles) (mean ± SEM; n= 4-6). (c) Expression of *G6pc1* relative to the respective littermate values (black circles) of I.G6pc$^{overexp\text{-}P1}$ and I.G6pc$^{overexp\text{-}c}$ mice (white circles) (mean ± SEM; n= 5-7). Two-way ANOVA, followed by multiple comparisons and Tukey's post hoc test were performed as statistical analyses.